BACHELOR THESIS

HEATING SOLUTION FOR A VARIABLE STIFFNESS SURGICAL MANIPULATOR

Jonathan Bos

SURGICAL ROBOTICS LAB
DEPARTMENT OF BIOMECHANICAL ENGINEERING
FACULTY OF ENGINEERING TECHNOLOGY
PROF. DR. S. MISRA

EXAMINATION COMMITTEE
PROF. DR. S. MISRA
DR. IR. M. MEHRPOUYA
T.L.THOMAS, PHD CANDIDATE

DOCUMENT NUMBER
FACULTY OF ENGINEERING TECHNOLOGY - BE-893

UNIVERSITY OF TWENTE.

OKTOBER
2022

Abstract

Minimally invasive surgeries are becoming more predominant as these surgeries require less invasive techniques than conventional surgeries. These minimally invasive surgeries require small incisions made in the body without increasing the size of the manipulator to be inserted inside and steered. Small manipulators can be made of smart materials such as shape memory materials. Shape memory polymer is an interesting material to use because its stiffness can vary depending on temperature. This thesis will look at different heating methods for use in an already existing design of a variable stiffness surgical manipulator made with shape memory polymer. Joule heating using nichrome wire will be expanded upon and modeled to characterize the thermal behavior of the heated shape memory polymer inside the prototype design. This is done in MATLAB R2021b and COMSOL Multiphysics 5.1. Experiments were conducted using the FLUKE Ti480 pro to verify the model and to evaluate if the heating method for heating the shape memory polymer variable stiffness manipulator is effective. The nichrome wire can effectively be used to heat the prototype for 30 seconds to a temperature of 60 °C. It takes approximately 200 seconds for the shape memory polymer to cool back down.

Contents

1 Introduction

Minimally invasive surgeries are becoming a popular treatment over traditional surgeries. These surgeries require a small incision to create an opening into the body for surgical equipment to enter the body. These surgeries often require multiple dedicated surgical tools to be inserted into the same incision. The downside of these surgeries are that the tools that are used are often rigid and can cause internal damage [1]. To minimize damage done to the inner walls of the vascular system flexible surgical robots made of smart materials are becoming more predominant [1]. An example of one of these flexible variable stiffness manipulators is shown in figure 1, where the body of the manipulator consist of a material that is either rigid or soft. This segmented manipulator can go around tight corners in its soft state and can squeeze through tight spaces while being rigid. A permanent magnet can be attached to the end of the flexible end-effector to steer it to the preferred location inside the body. The movement of this magnet can be controlled from outside the body via a magnetic field. This has the advantage that the size of the manipulator can be reduced so it allows the manipulator to move into smaller spaces. An example of this technique is shown in figure 1, where the manipulator made of a low melting point alloy.

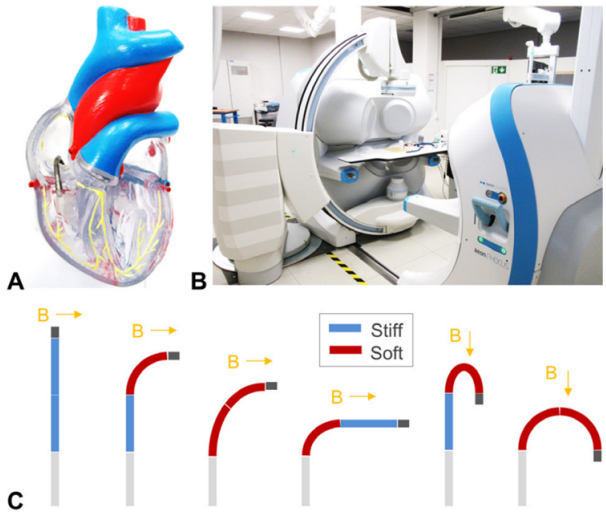

Figure 1: (A) A heart model to simulate surgery (B) Magnetic manipulation system used for testing magnetic manipulator (C) Flexible magnetic manipulator with variable stiffness segments made of low melting point alloy [2]

Another example of a variable stiffness manipulator is made of a material called shape memory polymer. By changing temperature conditions the the stiffness of the materials changes, such a design is shown in figure 2. In this design here is a inner hollow tube for housing surgical equipment surrounded by a variable stiffness polymer.

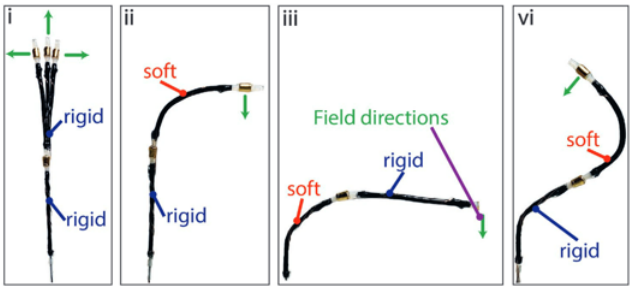

Figure 2: Flexible magnetic manipulator consisting of two segments that can be controlled individually [3]

Smart materials like the ones mentioned are becoming more predominant in the medical industry and show great potential [2]. Shape memory polymer (SMP) is one of these smart materials. This material can also change its characteristics depending on external factors. A variable stiffness catheter Made fo SMP will be expanded upon in this research. For making the SMP prototype manipulator there needs to be a way to activate the SMP. This can be done by integrating a heating element into the design. In the next chapters the design of one of these manipulators will be explained. This thesis will try to find a heating solution for the variable stiffness manipulator. After a sufficient heating mechanism is chosen it will be modeled to understand its behavior. This heating solutions will be modeled to determine the best parameters for practical use of the prototype. Simulations will be done to determine the temperature and the energy requirements to power the heating element and optimal settings for effective heating and cooling. To validate the model experiments will be done in which the thermal properties will be measured using a thermal imaging camera.

2 Background

2.1 Shape memory polymer

Shape memory polymers are part of larger group of shape memory materials [4]. These materials can be used in a wide range of biomedical applications such as drug delivery, stents and wound closure [5]. Some of the materials also have the potential to be used various other technical fields such as: smart structual repair, health monitoring, smart clothing and biosensors [6]. Shape memory polymers have a lot of advantages over other types of shape memory materials. Some types of SMP are bio-compatible with the human body. They are often easy to work with, come in different kinds of forms, pellet, 3dprint filament, resin and solution[4]. This makes them ideal candidates for the use in biomedical industry. There are several advantages of using shape memory polymers over for example shape memory alloys in medical devises. SMPs are lighter, have a higher recoverable strain and are often more cost effective. Some shape memory polymers are also biodegradable [7]

The mechanism that makes the shape memory effect possible is that the polymer consist of two segments. An elastic segment, and a transition segment. These segments can be chemically or physically connected. At low temperatures both of the segments are hard. When heated above the transition temperature the transition segment becomes soft. Figure 3 shows the change in elastic modulus depending on temperature. By deforming the polymer, elastic energy can be build up. When the polymer is cooled down again, the transition segment hardens. If constrains are added to the deformed shape when cooling it down the transition segments locks the elastic segment in place and elastic recovery can not take place. When the constrains are removed and the polymer is heated above its transition temperature, the elastic segment releases its energy and the polymer returns to the original shape [4] [7].

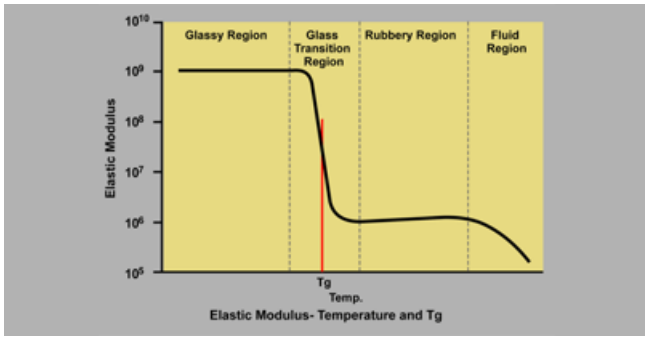

Figure 3: Characteristics of shape memory polymer. Elastic modulus changes depending on temperature [8]

When this polymer is treated under special conditions, the material can be fixated in a specific shape. When it is deformed to another shape, the material can stay that shape until an external stimulus is given to the material. Meaning the material 'remembers' the original shape it was trained in [9]. The he material has in essence two different states. The material can be in a hard, glassy state, or in a soft elastic state. The temperature at which this state change occurs is the glass-transition temperature. Figure 4 shows the mechanism of a SMP changing shape under temperature change, and returning to a previous shape once heated back up again.

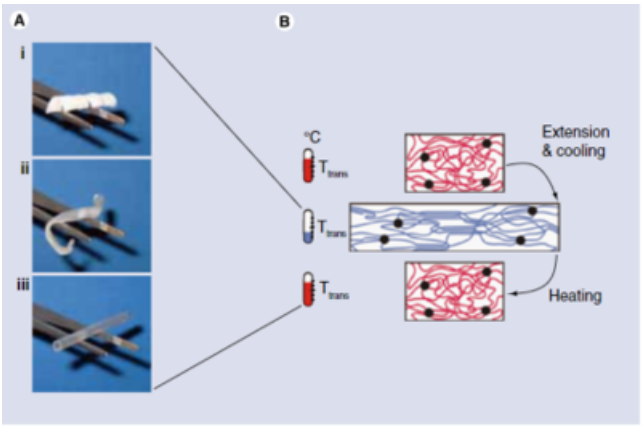

Figure 4: Shape-memory effect when reheated above glass transition temperature, the polymer returns to its pre-trained shape. [10]

There are many different types of shape memory polymer made from all kinds of polymers such as: polylactide, methancrylate polycaprolacone, acrylate based and Cyanocrylate based [11]. This thesis will focus on one particularly. Polyurethane shape memory polymer MP3510 from a company called SMP technologies Inc. This specific polymer has a glass transition temperature of 35 C. The chemical composition of this polymer is shown in figure 5.

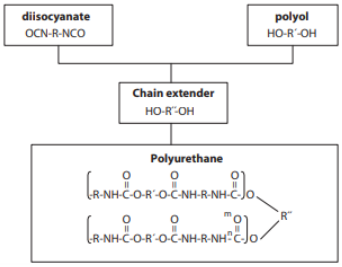

Figure 5: Molecular structure of polyurethane [12]

2.2 Design of variable stiffness manipulator

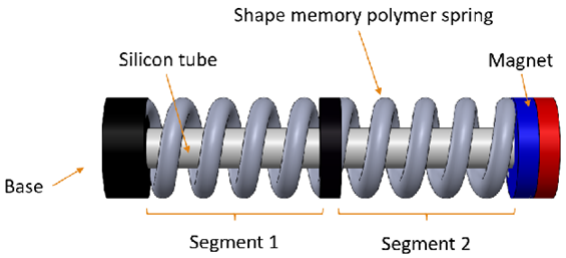

Figure 6: Design of variable stiffness manipulator made of shape memory polymer

The variable stiffness manipulator is made of two segments with a variable stiffness SMP spring around an inner silicone tube. The function of the inner tube is to expand and retract the spring to an extended and retracted shape respectively. The springs are connected using plastic connector pieces. A permanent magnet is attached to the end of the manipulator. The manipulator can be controlled by adding a changing external magnetic field to the system.

The spring sections of the prototype are an important part of the concept. These SMP springs are not only used for their spring capabilities but to offer variable stiffness so it bends when the SMP is in its rubbery phase and holds its shape when the SMP is in glass phase. The other advantage of the spring design is its ability to expand and retract when the SMP is in its rubbery state.

An important aspect of the design is when the SMP is heated all the SMP gets heated uniformly. When hot spots form on the surface of the SMP it may cause damage to the structure of the prototype. Another important part in the prototype design is the inner silicon tube. This tube makes it possible for the electrical components to stay inside the prototype, and make sure the prototype retains its structural integrity.

The specific SMP type is from SMP Technologies Inc. and will be used in the prototype. They offer different types of polyurethane SMPs, with different glass transition temperatures. Ranging from 25 to 55 °C. When choosing the best type of SMP. Since the prototype is intended to be used inside the body. The range in glass transition temperature is limited. It can not be to low because then the internal heat of the body will heat the SMP enough to trigger its shape memory effect. If the temperature is too high it may cause damage to the interior of the body. Since internal body temperature is around 37 °C, the SMP will be in its glass transition region. By adding a heat source the temperature of the SMP can be increased to be in the rubbery region.

3 Heating methods

The SMP in the prototype must be heated to activate its shape changing properties. Therefore a heating solution must be found, which satisfies the following criteria.

- It must fit into the design without any extra hindrance.
- It must effectively heat the SMP without letting too much heat leak into the surrounding area.
- The heating solution must be compatible with integration in current medical equipment.

Taken these criteria into consideration three heating options are considered. Joule heating, Peltier heating and laser optic fiber heating, which will be discussed in this section

3.1 Joule heating

Joule heating is the process where heat is generated by passing a current through a resistance wire. Different materials can be used to utilize this effect. One of the common materials used for heating is nichrome. This material is commonly used in electric heaters and toaster because it has a high resistivity and is resistant to oxidation [13] [14]. The advantage of using this option is that the wire can be connected to a power source and because of its small form factor it can integrated into the prototype design. To maximise effective heating the thickness of the wire can be changed depending on the necessary heat required for heating the surrounding SMP.

3.2 Peltier effect

A thermoelectric heating unit can be used to generate the heat for heating the shape memory polymer. The peltier effect generates a temperature difference between the junction of two semiconductors: P-type and N-type. P-type semiconductors have impurities added to create electron vacancy. N-type semiconductors have impurities added to create extra electrons. When a current is passed through these semiconductors electron flow takes place at the junction of these semiconductors. This electron flow results in a temperature difference. This current can be turned around to create opposite effect as well. This heating option has the advantage of also being able to cool the SMP down after heating [15]. A thermoelectric circuit is shown in figure 7, where the current can be reversed to switch between cooling and heating. The disadvantage of using this technique is the large form factor of the peltier heating element.

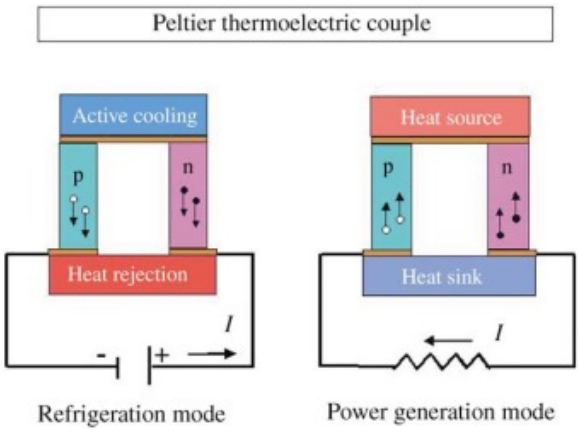

Figure 7: Peltier effect in theromoelectric circuit[15]

3.3 Laser fiber optics

A fiber optic cable can be used to heat the SMP by embedding an optical fiber into the SMP and adding a diode laser into the design of the SMP spring. Some of the light generated by the diode gets absorbed by a coating on surface of optic fiber and radiates heat to surroundings. This photo thermal effect can be used to heat the SMP. Different substances such as, gold nano-particles, graphine or carbon black can be added to the optical fiber to increase the heat dissipation into the surrounding SMP [16]. In figure 8, an optical fiber encased in SMP is shown where the laser heats the coated fiber optic cable.

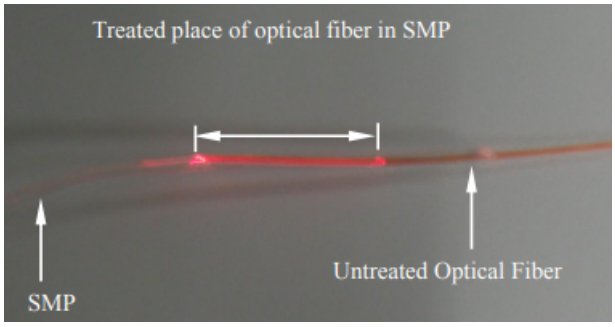

Figure 8: Optic fiber laser heating in SMP [17]

3.4 Heating solution

The advantages and disadvantages of each solution are summarized table 1. Joule heating is found to be the most feasible option for integration in the variable stiffness manipulator. This method of heating the SMP can easily be integrated into the design. Because of the small form factor of the wire it can be integrated into the design. By adding a internal nichrome wire going back and forth on the inside of the SMP it can be heated uniformly. By making both ends of the wire come out of the same side the heating can be controlled from one end of the manipulator. This method of integrating the wire is shown in figure 9.

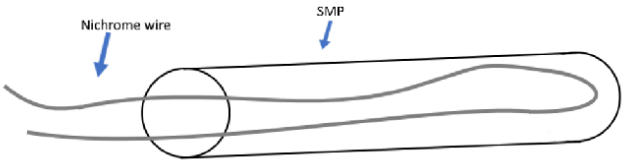

Figure 9: Visual representation nichrome wire inside silicone tube

Table 1: Pros and cons for each heating method

Heating solution	Advantages	Disadvantages
Joule heating	Small form factor Uniform heating	Risk of overheating
Peltier effect	Heating and cooling	Large form factor Inefficient energy consumption
Laser	Small form factor	Equipment integration cost Light escapes and heats surroundings[18]

4 Methods

4.1 SMP prototype design and fabrication

As a heating solution a nichrome wire is chosen. The variable stiffness actuator is controlled from one end. Both ends of the nichrome wire need to be on the same side of the prototype this means the nichrome wire has to be electrically insulated otherwise it can short itself and cause uneven heating of the SMP. To solve this problem the nichrome wire can be coated in with an electrical insulating spray before being inserted into the silicone mould. The spray used is Kontakt Chemie Transparent Urethan 71 Aerosol PCB Coating. This process is shown in figure 10A.

The type of SMP for making the protoype is the potting type. Consisting of a resin and a hardener. When mixed together the mixture thickens within 5 minutes. To reduce air bubbles in the mixture the resin and hardener are treated in a vacuum chamber for 2 hours. When the hardener and resin are mixed they quickly thicken and turn in to a hard solid if placed in and oven at 70 C for 1 to 2 hours. This way of making the SMP allows for injection into any mould. To achieve the required spring shape first a cylinder shaped rod has to be made. This can be done by injecting the resin and hardener mixture into a silicon tube with an inner diameter of the preferred SMP diameter. After the SMP is cured the silicone can be removed by cutting it away.

The next step to add a protective housing over the exposed nichrome wires. This step is also very important because the exposed wires can get hot quickly and cause damage to the prototype. A small silicon tube with a injection of Ecoflex™ liquid silicon can be put over the exposed wires to thermally insulate them. This proces is shown in figure 10C.

To train the SMP into the desired shape a 3d printed mould is used. The SMP is shaped into a spring by wrapping it around a bolt with an diameter of 4mm and clamping it down with a mould. This mould shown in figure 10E consist of two plastic parts held together by screws. The mould constrains the SMP rod into a spring shape. The SMP in its mould is kept in the oven for 16 hours at 70 °C. After this training period the SMP stays the same shape even after heating it above its glass transition temperature. The final spring will be used in the prototype design.

4.2 Model

4.2.1 Steady state

The thermal behavior of the SMP spring can be modeled as a straight rod that is cylindrical in shape. For calculation the temperature of the SMP, the system will be modeled as a thermal resistance network. The network consist of a conduction resistance for the transfer between the nichrome and SMP and a convection resistance on the outer surface of the SMP. There are two wires in a cross-section but for modeling the temperature distribution the area of those two wires will be simplified to one wire of an equal area. This simplified representation is shown in figure 11.

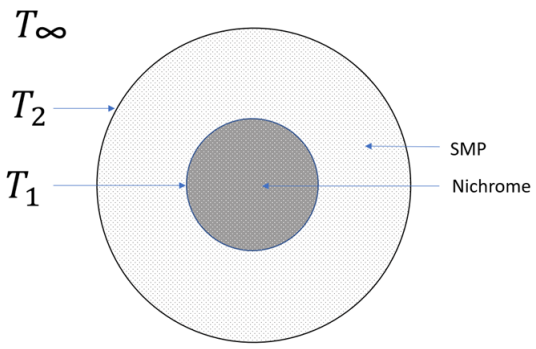

Figure 11: Simplification wire cross-section nichrome wire surrounded by SMP

$$Q = I^2 R \tag{1}$$

The energy generated depends on the intensity of the current that is flowing through the nichrome wire following Watts law. This energy generated from this phenomenon is called joule heating, calculated by equation (1). I is the current passed thought a wire with a resistance Re.

A thermal resistance network consisting of a resistance from conduction through the SMP layer and the resistance from convection is shown in figure 12

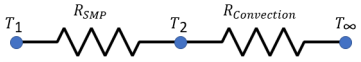

Figure 12: Visual representation thermal resistance network

$$R_{SMP} = \frac{ln(r2/r1)}{2\pi kL} \tag{2}$$

$$R_{convection} = \frac{1}{hA} \tag{3}$$

$$T_1 = T_\infty + Q(R_{SMP} + R_{convection}) \tag{4}$$

The thermal resistance network can be modeled by equations (1-4), where r1 and r2 are the radii of the nichrome wire and SMP shell surrounding it, A the surface area, k the thermal conductivity of SMP , L the length of the SMP rod and h the convective heat transfer coefficient.

$$T_2 = T_1 - \frac{E_{gen} r_1^2}{2k_{SMP}} (\log \frac{r_2}{r_1}) \tag{5}$$

The temperature difference between T_1 and T_2 can be modeled. By assuming there is constant heat generation by means of Joule heating following equation(1) and heat transfer from r1 to r2. E_{gen} in this equation is the energy density that is produced by the Joule heating[19].

Table 2: Material properties nichrome and polyurethane SMP

Parameter	Value
Density nichrome	8400 kg m^3
Density SMP	1100 kg m^3[20]
Thermal conductivity nichrome	11.3 W $m^{-1}K^{-1}$[21]
Thermal conductivity SMP	0.51 W $m^{-1}K^{-1}$[20]
Thermal diffusivity SMP	0.12x$10^{-3}m^2s^{-1}$[20]
Convective heat transfer coefficient	5-25 W $m^{-2}K^{-1}$[22]

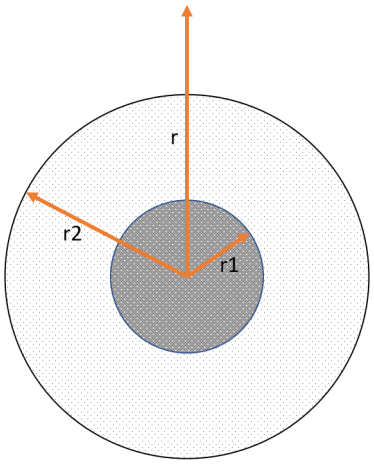

Figure 13: Simplification cross-section model

4.2.2 Time dependent

The polymer rod consist of two materials. An inner nichrome core and a SMP insulating layer. Since the rod is symmetrical along its radial axis, the one dimensional heat equation can be applied to calculate the heat transfer over time. By adding two boundary constraints, one for the internal heat generation by Joule heating and one boundary condition for the loss of heat to the surrounding area the system can be modeled[23].

$$\frac{\partial T}{\partial t} = a_0 \frac{1}{r} \frac{\partial \left(\lambda_0 r \frac{\partial v}{\partial t}\right)}{\partial r} = a_0 \left(\frac{\partial T}{\partial t} \frac{1}{r} + \frac{\partial^2 T}{\partial r^2} \right) \tag{6}$$

$$T(r,0) = T_\infty \qquad r1 \leq r \leq r2 \tag{7}$$

$$\frac{\partial T}{\partial r} = \frac{I^2 R}{2r\pi\lambda_0} \qquad (r = r1) \tag{8}$$

$$\frac{\partial T}{\partial r} = \frac{h\left(T - T_\infty\right)}{\lambda_0} \qquad (r = r2) \tag{9}$$

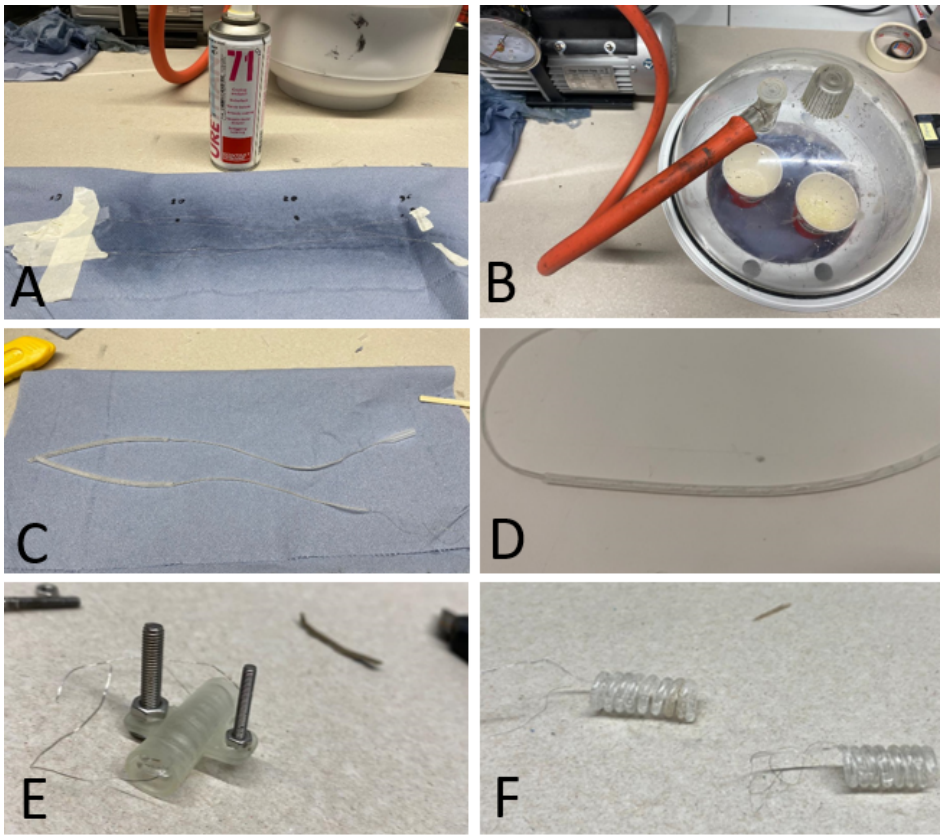

Figure 10: SMP spring fabrication process. A: Urethane coating on the nichrome wires for electrical insulation. B: Vacuum treating of the resin and hardener of the SMP potting type. C: Ecoflex™ liquid silicon injection into the silicone tube. D: SMP rod encapsulated by silicone tubing. E: SMP rod restrained into spring shape F: Final spring shape

The one dimensional heat equation is shown with its initial and boundary conditions in equation(6-9). The inner and outer radii r1 and r2 of the nichrome wire and SMP insulating layer respectively, this is shown in figure 13. a_0 is the insulation thermal diffusivity, λ_0 the insulation thermal conductivity, I current density, R resistance of the nichrome wire and h the surface heat transfer coefficient. This heat transfer coefficient is not a material property but depends on geometry and airflow around the object. By adding parameters the temperature change over a selected time period can be modeled in MATLAB.

4.3 Experiment

The experiments were done with the FLUKE ti480 thermal imaging camera. The surface temperature of the SMP with integrated nichrome wire was measured over a set period of time. First the nichrome wire is connected to the power supply to measure how fast the SMP is heating up and than the power supply is turned of to record the cooling time of the SMP. The experimental setup of this experiment is shown in figure 15. The thermal camera is held in place using a vice grip. The nichrome wires are connected to a power supply with variable current shown in figure 14. Other experiments are also done to determine optimal conditions for making the SMP spring that will be used in the prototype. First an experiment is done to determine the optimal thickness of the SMP layer. In this experiment the radius of the rod will be varied. In the second experiment the different shapes of the SMP are measured, where the straight SMP rod will be compared to the SMP spring shape. After the two experiments the flexible manipulator prototype will be heated by nichrome wire and the temperature change will be measured.

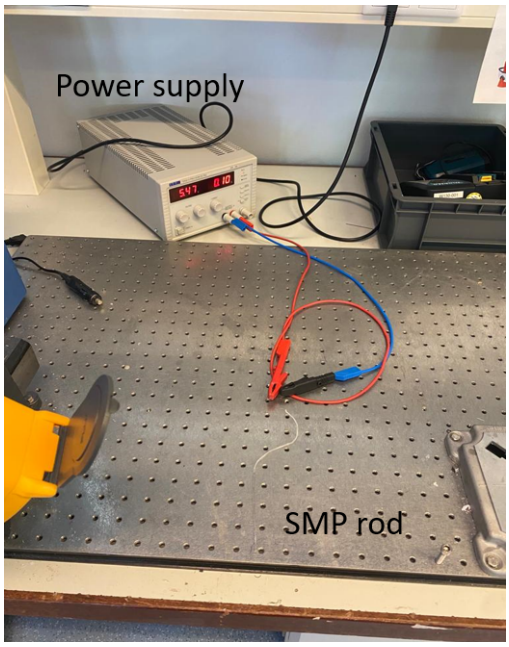

Figure 14: Experimental setup nichrome wires connected to a power supply

Figure 15: Experimental setup measuring temperature of SMP rod.

5 Results

5.1 Steady state

The steady state temperature distribution is modeled in COMSOL. The simulation is done in 2 dimensions. As The two wires are modeled as a constant heat source, with surface heat transfer to the surrounding material and convection cooling on the outer surface of the circle. All the material properties of nichrome and polyurethane are added to the model for the simulation. A normal size mesh is generated. In this simulation the nichrome wires can be modeled in two separate wires, which more realistically represents the actual prototype. This is done by simulating Joule heating by the nichrome wires and adding the physics for heat transfer in solids for nichrome and SMP. The heat generated dissipates via convection cooling so this is also added to the simulation.

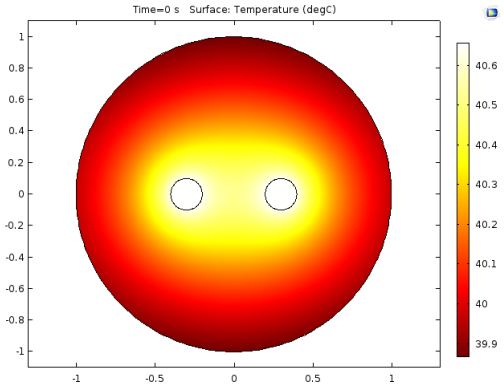

Figure 16: COMSOL simulation of temperature distribution when 0.1 A current is supplied through two nichrome wires

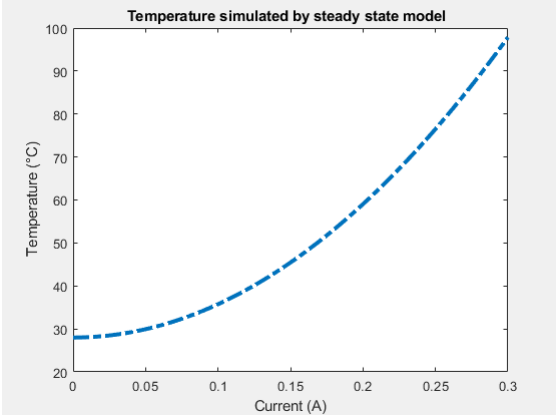

Figure 17: Steady state surface temperature of different current values

5.2 Time dependent

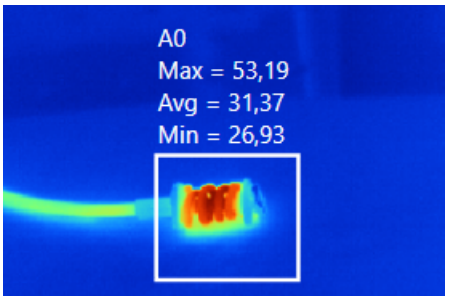

Figure 18: Thermal image of a segment of the prototype heated by nichrome wire

To analyse the temperature data the maximum temperature of each thermal image frame is taken. This data was gathered by exporting all the frames and plotting the temperature values against the time scale. Figure 18 shows a frame of a measurement when the SMP is heating up. It shows the spring getting the hot and the nichrome wire on the left side being cooler than the exposed SMP.

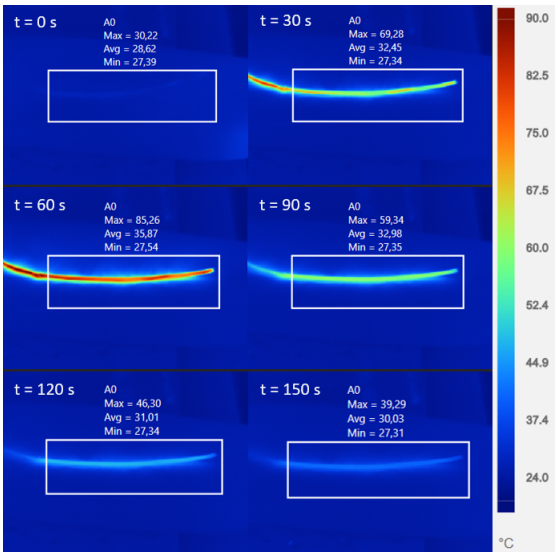

Figure 19: Snapshots of measurements at time intervals of 30 seconds, 0.2 A current supplied for 62 seconds.

Figure 19 shows the temperature change of a SMP rod with integrated nichrome heating wire. The wire is heated for 62 seconds by the integrated nichrome wire at a current of 0.2 A. In the second stage the SMP rod cools down to room temperature.

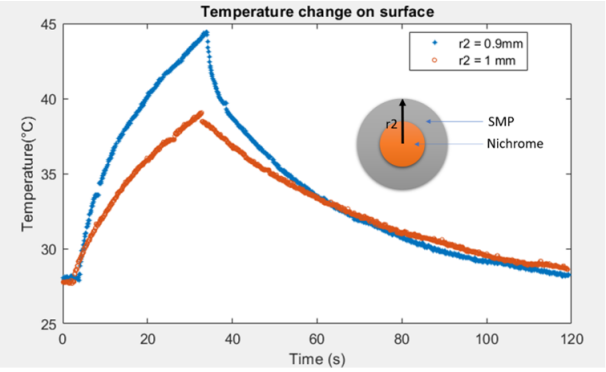

Figure 20: Thermal behavior of SMP with different thicknesses SMP layer

Figure 20 shows the maximum temperature of the SMP rod changing over time. The SMP with the smaller radius heats up and cools down faster.

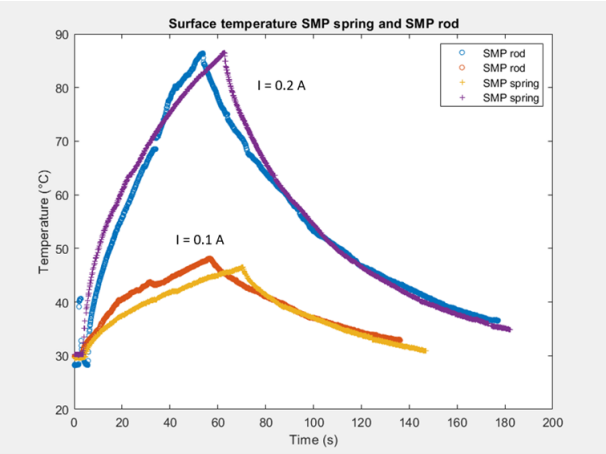

Figure 21: Thermal behavior of SMP spring and SMP rod at 0.1 A and 0.2 A

In figure 21 the results of a temperature measurement of a SMP rod are shown next the temperature data from the SMP spring. As seen in the figure it takes the SMP prototype a longer time to reach the same temperature. However the SMP spring with a 0.2 A current heating up faster than SMP rod in the first 30 seconds.

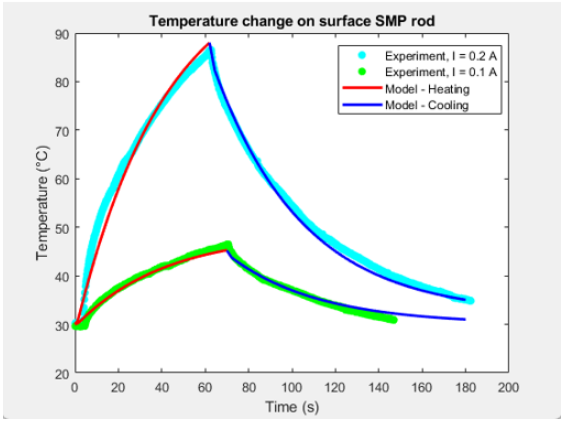

Figure 22: Comparison model with experimental data where one SMP rod is heated by passing 0.2 A current and 0.1 A current through the nichrome wire. After 60 s the current is turned of and the temperature lowers

s

When the starting conditions and heating time are known the model predicts the experimental data. For this simulation a convection coefficient of 30 W/m^{2}K is chosen.

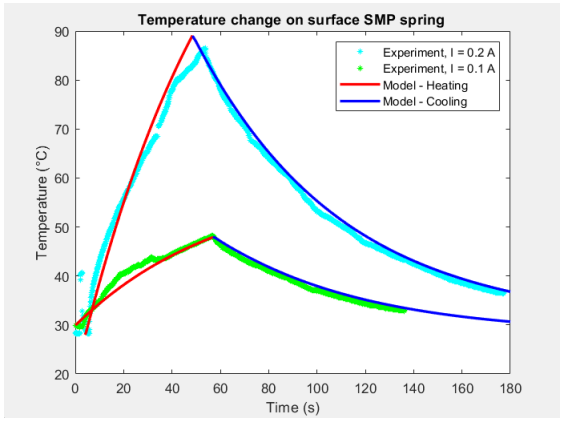

Figure 23: Comparison model with experimental data were one SMP spring is heated by passing 0.2 A current and 0.1 A current through the nichrome wire. After 60 s the current is turned of and the temperature lowers

Figure 23 shows the experimental results of heating the SMP spring with the nichrome wire at a current of 0.1 A and 0.2 A. This simulation differs from the SMP rod simulation in its convective heat transfer coefficient, h is 20 W/m^{2}K. The heating phase starts later in the experiment where the wire is heating with 0.2 A nichrome wire, this is also adjusted in the model.

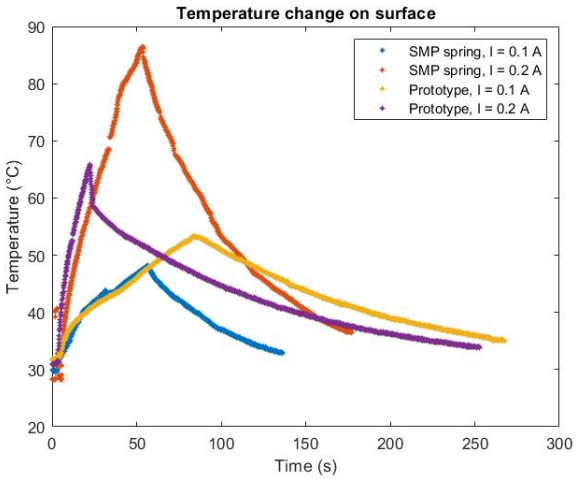

Figure 24: SMP spring compared against prototype when heated with a nichrome wire with current of 0.1 and 0.2 A

Figure 24 shows the change in maximum temperature on the surface of a SMP spring and a SMP spring integrated into the prototype design. Different heating times are applied to the SMPs. The graph shows that the prototype is behaving similar in the heating phase but its taking longer to cool down close to room temperature. When comparing the prototype to the SMP spring at 0.2 A the SMP spring is faster in cooling down to room temperature than the prototype.

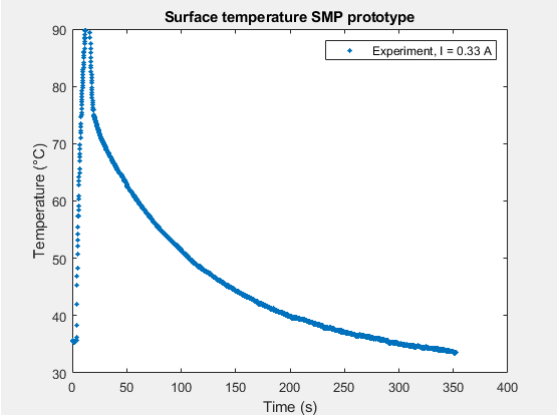

Figure 25: Experimental temperature measurement of SMP prototype heated by nichrome wire with a current of 0.33 A for a few second

An experiment was done to determine the upper limits of the SMP prototype. Figure 25 shows the change in surface temperature when the SMP is heated fast with a current of 0.33 A. The maximum temperature of the SMP prototype is over 90 C and reached the maximum temperature measurable by the thermal imaging camera.

6 Discussion

6.1 Model validation

6.1.1 MATLAB

The steady state model predicts the temperature of the SMP when an equilibrium is reached. In this equilibrium the energy generated by joule heating is dissipated into the environment by convection cooling. As seen in figure 17 the optimal temperature of 60 °C is reached at around 0.2 A. From the experimental results it is clear that the SMP reaches these temperatures at a lower current.

As seen in figure 22 the model can predict the thermal behavior of the SMP rod. It can predict the heating and cooling time under different conditions. There are two different models for determining the temperature of the SMP, one for heating and one for cooling. These models could be combined into one model.

6.1.2 COMSOL

The COMSOL simulation predicts lower steady state outside temperature than experimentally measured. This temperature distribution is also more comparable to the steady state thermal resistance model. As seen in the figure 21 the SMP reaches over 45 °C, and it still has not reached its steady state temperature. This higher temperature of the SMP rod is not reflected in the steady state model. The difference in thermal behavior might arise from fact that the COMSOL simulations have been done with the material properties of polyurethane and not the thermal properties of polyurethane SMP.

6.2 Design assessment

The optimal conditions for the SMP reaching 60 °C can be achieved by heating the SMP with an internal nichrome wire. At 60 °C the SMP is fully in the rubbery phase. To reach this temperature a current of 0.18 A can be applied for 30 seconds. The SMP would take approximately 200 seconds to cool down again going back to a glassy state. It would be advantageous if the SMP is heated faster by applying a higher current for a shorter time. The experimental results from figure 25 shows that the SMP reaches a temperature of 90 °C within 10 seconds. This heating time is within reasonable timescales for practical use, however the cooling phase takes around 5 minutes.

The temperature of the SMP can be too high and cause unsafe situations. Tissue damage takes place after 3 seconds at 62 °C [24]. To solve this problem the prototype can be more insulated.When the silicone tube is not removed from the SMP it will insulate the rod more. As seen in figure 26 the surface temperature is greatly reduces with the extra insulation since the thermal camera is only measuring surface temperature the actual temperature of the SMP is unknown. This extra insulation might help the SMP get to higher temperatures without adding any risk of causing internal damage to the body. The disadvantage of insulating the SMP this way is that it might take longer for the SMP to reach its glassy state again.

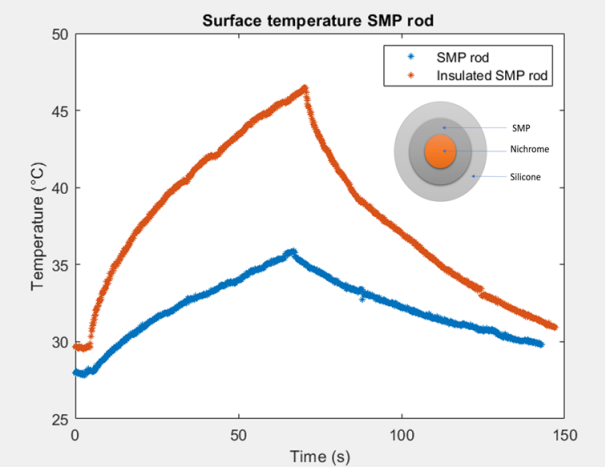

Figure 26: Thermal behavior of the same SMP rod with and without silicone cover

Two different nichrome wires were used in making the prototypes, 0.12 mm and a 0.06 mm wires. The thinner nichrome wire often broke in the process in making the prototypes or when the wires were connected to the power supply. For these reasons the SMP rods with the thinner nichrome wire were not experimentally tested.

The thinner SMP layer heats up and cools down faster. It is unclear if this smaller radius influences the structural integrity of the variable stiffness actuator. further research needs to be done to determine the optimal SMP layer thickness. When looking at the total cooling time the initial temperature has to be considered, the SMP takes longer to cool down if its hotter. As seen in table 3 the cooling down time of the prototype is significantly longer than the time it takes for the SMP rod and spring to cool down. Heating times are dependent on the current passing through the nichrome wire and faster heating is more beneficial. The convection coefficient changes depending airflow over the surface. All the simulations and experiments were done with the assumption that the manipulator was exposed to free flowing air. The convection coefficient depends on flow conditions ad geometry [25]. If the SMP is in a spring shape less airflow will be able to go over every coil of the spring, resulting in less heat being transported. In the prototype design this airflow over the surface will be even more reduced, thus increasing the convection coefficient. When using the manipulator for its intended use inside the body the heat transfer will be different. To measure the effect of this different environment another experiment has to be done.

Table 3: Cooling down times of different SMP shapes. when cooled down from 45 °C to 35 °C

SMP	**Cooling time 0.1 A**	**Cooling time 0.2 A**
Rod	40.4 s	53.8 s
Spring	50.3 s	54.9 s
Prototype	127.6 s	124.2 s

6.3 Future work

In this research only one type of SMP is used. For future research multiple kinds of SMP can be tested get a better understanding in which SMPs can be used for similar purposes, there might be an alternative SMP with better thermal qualities. A smp with a glass transition region ranging from 40 °C to 50 °C could be more functional in the manipulator, since the SMP can fully cool down to its glassy state. Another topic that can be be searched upon more is the mechanical behavior of the SMP under different temperatures conditions.

7 Conclusion

This study focused on finding a viable heating solution current state of flexible variable stiffness manipulators. By integration the nichrome wire into the design the surrounding SMP can be heated. Joule heating was chosen as the heating method for heating the SMP to above its glass transition temperature. Mainly for its fast heating and integration in existing work environments. Temperature can be controlled with high accuracy, which makes it a good candidate for experimental measurements. The parameters in the time-dependent model can be adjusted to predict the heating and cooling time of future prototypes. The model can predict the temperature change of the SMP. The variable stiffness manipulator can reach the desired temperature making use of its shape memory effect within 10 seconds. This is within reasonable time scale for the use in surgeries, however the cooling down time to below the SMPs glass transition temperature takes up to 2 minutes. This cooling down time however will change drastically when used inside the body since fluids have a higher convective heat transfer coefficient. This still has to be experimentally tested. The variable stiffness manipulator can be used as end-effector of many different applications. The manipulator has the potential be used for colonoscopies. Its size and variable stiffness allow the manipulator to make tight corners resulting in easier steering to harder to reach places.

References

[1] T. Ranzani, M. Cianchetti, G. Gerboni, I. De Falco, and A. Menciassi, "A soft modular manipulator for minimally invasive surgery: design and characterization of a single module," *IEEE Transactions on Robotics*, vol. 32, no. 1, pp. 187–200, 2016.

[2] C. Chautems, A. Tonazzini, D. Floreano, and B. J. Nelson, "A variable stiffness catheter controlled with an external magnetic field," in *2017 IEEE/RSJ International Conference on Intelligent Robots and Systems (IROS)*. IEEE, 2017, pp. 181–186.

[3] Y. Piskarev, J. Shintake, C. Chautems, J. Lussi, Q. Boehler, B. J. Nelson, and D. Floreano, "A variable stiffness magnetic catheter made of a conductive phase-change polymer for minimally invasive surgery," *Advanced Functional Materials*, p. 2107662, 2022.

[4] W. M. Huang, B. Yang, and Y. Q. Fu, *Polyurethane shape memory polymers*. CRC press Boca Raton, FL, 2012.

[5] G. I. Peterson, A. V. Dobrynin, and M. L. Becker, "Biodegradable shape memory polymers in medicine," *Advanced healthcare materials*, vol. 6, no. 21, p. 1700694, 2017.

[6] P. T. Mather, X. Luo, and I. A. Rousseau, "Shape memory polymer research," 2009. [Online]. Available: www.annualreviews.org

[7] H. W. D. Z. W. CC, "Wei j. zhao y. purnawali h," *Mater. Today*, vol. 13, pp. 54–61, 2010.

[8] SMPtechno, "News." [Online]. Available: http://www.smptechno.com/index_en.html

[9] M. Rubinstein, R. H. Colby *et al.*, *Polymer physics*. Oxford university press New York, 2003, vol. 23.

[10] A. Lendlein and S. Kelch, "Shape-memory polymers," *Angewandte Chemie International Edition*, vol. 41, no. 12, pp. 2034–2057, 2002.

[11] S. Basak, "Redesigning the modern applied medical sciences and engineering with shape memory polymers," *Advanced Composites and Hybrid Materials*, vol. 4, no. 2, pp. 223–234, 2021.

[12] W. M. Huang, B. Yang, and Y. Q. Fu, *Polyurethane shape memory polymers*. CRC press Boca Raton, FL, 2012.

[13] D.-H. Im, T.-W. Yoon, W.-S. Min, and S.-J. Hong, "Fabrication of planar heating chuck using nichrome thin film as heating element for pecvd equipment," *Electronics*, vol. 10, no. 20, 2021. [Online]. Available: https://www.mdpi.com/2079-9292/10/20/2535

[14] I. Naseri, M. Ziaee, Z. N. Nilsson, D. R. Lustig, and M. Yourdkhani, "Electrothermal performance of heaters based on laser-induced graphene on aramid fabric," *ACS Omega*, vol. 7, no. 4, pp. 3746–3757, 2022.

[15] T. M. Tritt and M. A. Subramanian, "Thermoelectric materials, phenomena, and applications: A bird's eye view," *MRS Bulletin*, vol. 31, no. 3, p. 188–198, 2006.

[16] M. Herath, J. Epaarachchi, M. Islam, F.-h. Zhang, L. Jinsong, L. Fang, C. Yan, G.-D. Peng, and W. Schade, "Remote actuation of light activated shape memory polymers via d-shaped optical fibres," *Smart Materials and Structures*, vol. 29, 02 2020.

[17] D. Zhang, Y. Liu, and J. Leng, "Infrared laser-activated shape memory polymer," in *Sensors and Smart Structures Technologies for Civil, Mechanical, and Aerospace Systems 2008*, M. Tomizuka, Ed., vol. 6932, International Society for Optics and Photonics. SPIE, 2008, p. 693213. [Online]. Available: https://doi.org/10.1117/12.776109

[18] W. S. IV, T. S. Wilson, W. J. Benett, J. M. Loge, and D. J. Maitland, "Laser-activated shape memory polymer intravascular thrombectomy device," *Opt. Express*, vol. 13, no. 20, pp. 8204–8213, Oct 2005. [Online]. Available: http://opg.optica.org/oe/abstract.cfm?URI=oe-13-20-8204

[19] Y. Cengel and A. Ghajar, "Heat and mass transfer: Fundamentals and applications."

[20] B. Weidenfeller and M. Anhalt, "Polyurethane-magnetite composite shape-memory polymer: Thermal properties," *Journal of Thermoplastic Composite Materials*, vol. 27, pp. 895–908, 10 2014. [Online]. Available: https://journals.sagepub.com/doi/10.1177/0892705712458446

[21] "Gage awg diameter inch resistance at 68 f Ω/ft." [Online]. Available: www.resistancewire.com

[22] M. Malekan, A. Khosravi, and M. E. H. Assad, "Parabolic trough solar collectors," *Design and Performance Optimization of Renewable Energy Systems*, pp. 85–100, 1 2021.

[23] X. J. Li, J. Yang, B. Q. Yan, and X. Zheng, "Insulated cable temperature calculation and numerical simulation," *MATEC Web of Conferences*, vol. 175, 7 2018.

[24] D. Li, Y.-L. He, and G.-X. Wang, *Thermal Modelling for Laser Treatment of Port Wine Stains*, 09 2011.

[25] N. Gao, J.-S. Jeon, and D. E. Hodgson, "Transformation strain based method for characterization of convective heat transfer from shape memory alloy wires you may also like an innovative seismic bracing system based on a superelastic shape memory alloy ring," 2010.

8 Appendices

This appendix contains the MATLAB code for the steady state and time depending model, also included is the MATLAB code for processing the FLUKE thermal imaging camera data.

8.1 MATLAB code

8.1.1 Steady state

```
clear,
clc,
close all

%% constants

d = 0.12 *10^-3 ;                   % Diameter wire
L = 0.6          ;                  % Length wire
pi = 3.1415 ;
A = pi *( (0.5* d)^2);              % Surface crossection wire
p = 1.1 * 10^-6  ;                  % Resisivity nichrome
Tair = 28         ;                 % Temperature surroundings in Celcius
I = [0:0.001:0.3];                  % Range of I
%I = 0.15;                          % Current in ampere
knich = 11.3       ;                % Thermal conductivity nichrome W/m k
ksmp = 0.17;                        % Thermal conductivity smp in W/ m k
h = 25          ;                   % Convection coeficient in w/ m^2 k
r = [0:0.001:(0.12*10^-3)];         % Range of r
r1 = 0.12 * 10^-3;
r11 =sqrt(2*r1^2) ;                 % Radius nichrome wire
r2 = 1 * 10^-3 ;                    % Radius smp
Ab = 2*pi*r2*L;                     % Surface area


%% heat generation in simple nichrome wire (not insulated)
%Tememperature difference calculated via Joule heating
Re = (p .* L) ./ A;                 % Resistance
Q = I.^2 *Re   ;                    % Energy generated by joule heating
Egen = Q./(pi.* r11.^2 * L);        % Energy generated in wire (W/m3)
dT =  (Egen.*(r1.^2))./ 4*knich;        % Temperature difference inside wire and
    surface wire
%% conductive resistance
%Surface temperature calculated via thermal resistance network
Rconv = 1./(h* Ab);                                             % Convection heat
    resistance
Rpolymer = (log(r2./r11))./(2*pi*ksmp*L);                       % Conductive heat
    resistance
Tin = Tair + Q.*(Rconv + Rpolymer)    ;                         % Temperature on
    boundary layer
Tsurface = Tin - ((Egen.*(r1.^2))./2*ksmp) * log(r2./r1);       % Surface
    temperature

plot(I,Tsurface,'-.')
```

8.1.2 Time dependent

```
%% Heating
global lambda p0 specificHeat a0 r1 h I  R T0 rho crossarea r11 r2
```

```
lambda = 0.17;          %Thermal conductivity of SMP: Weidenfeller et al.
p0 = 1100;              %Density of SMP: Weidenfeller et al.
specificHeat = 2400;    %Specific heat of SMP
rho = 1.1 * 10^-6   ;   %Resistivity of nichrome

a0 = 0.12e-6;           %From paper Weidenfeller et al.
r1 = 0.12*1e-3;         %Radius nichrome wire
r11 = sqrt(2*r1^2);     %Effective radius of two wires
r2 = 1e-3;              %Radius SMP
h = 30 ;                %Convection constant
I = 0.18 ;              %Current
R = 60;                 %Resistance from experimental data
T0 = 24;                %Initial temperature
T1 = 50;
crossarea = 2*pi*r1^2;

x = linspace(r11,r2,100);
t = linspace(0,40,100);

m = 0;
sol = pdepe(m,@heatcyl,@heatic,@heatbc,x,t); %Solves partial differential
    equation with boundary conditions

u = sol(:,:,1);
%figure(1)
%surf(x,t,u)
%xlabel('x')
%ylabel('t')
%zlabel('u(t,x)')


plot(t,u(:,100),LineWidth=2,Color='r')  %plots temperature over time on r = r2
hold on

xlabel('Time (s)')
ylabel('Temperature ( C )')
title('Temperature change on surface')
legend('Model')
function [c,f,s] = heatcyl(x,t,u,dudx)
global  a0
f = dudx;
s = 1/x;
c = 1/(a0);
end

%Initial condition
function u0 = heatic(x)
global  T0
u0 = T0;
end

%Boundary condition
function [pl,ql,pr,qr] = heatbc(xl,ul,xr,ur,t)
global lambda r11 h I R T0
  pl = I^2*R/(2*r11*pi*lambda);
  ql = 1;
  pr =  h*(ur-T0)/lambda;
  qr = 1;
end

%% Cooling
```

```
global lambda p0 specificHeat a0 r1 h I  R T0 rho crossarea r11 r2
lambda = 0.17;          %Thermal conductivity of SMP: Weidenfeller et al.
p0 = 1100;              %Density of SMP: Weidenfeller et al.
specificHeat = 2400;    %Specific heat of SMP
rho = 1.1 * 10^-6  ;    %Resistivity of nichrome

a0 = 0.12e-6;           %From paper Weidenfeller et al.
r1 = 0.12*1e-3;         %Radius nichrome wire
r11 = sqrt(2*r1^2);     %Effective radius of two wires
r2 = 1e-3;              %Radius SMP
h = 30 ;                %Convection constant
I = 0 ;                 %Current
R = 60;                 %Resistance from experimental data
T0 = 24;                %Initial temperature
T1 = 50;
crossarea = 2*pi*r1^2;

x = linspace(r11,r2,100);
t = linspace(0,40,100);

m = 0;
sol = pdepe(m,@heatcyl,@heatic,@heatbc,x,t); %Solves partial differential
    equation with boundary conditions

u = sol(:,:,1);
%figure(1)
%surf(x,t,u)
%xlabel('x')
%ylabel('t')
%zlabel('u(t,x)')


plot(t,u(:,100),LineWidth=2,Color='r')  %plots temperature over time on r = r2
hold on

%plot(t,u(:,50))
xlabel('Time (s)')
ylabel('Temperature ( C )')
title('Temperature change on surface')
legend('Model')
function [c,f,s] = heatcyl(x,t,u,dudx)
global  a0
f = dudx;
s = 1/x;
c = 1/(a0);
end

%Initial condition
function u0 = heatic(x)
global  T1
u0 = T1;
end

%Boundary condition
function [pl,ql,pr,qr] = heatbc(xl,ul,xr,ur,t)
global lambda r11 h I R T0
  pl = 0;
  ql = 1;
  pr =  h*(ur-T0)/lambda;
  qr = 1;
end
```

Experiment data

```
clear, clc, close all
%% Data extraction from .xls files that are imported from the FLUKE .IS3
    temperature data
[files,path]=uigetfile('*.xls','multiselect','on');
for i=1:length(files)
[~,~, data{i}]=xlsread(fullfile(path,files{i}));
maxtemp(i) = str2double(data{i}(5,6));              %change acording to max temp
    location in excel file.
end
plot(((1:length(maxtemp))*0.111),maxtemp)
```